

NATIONAL RADIO ASTRONOMY OBSERVATORY  
CHARLOTTESVILLE, VIRGINIA

ELECTRONICS DIVISION INTERNAL REPORT No. 282

43 GHz, COOLED, LOW-NOISE AMPLIFIER

S. WEINREB, R. HARRIS, AND M. ROTHMAN

DECEMBER 1988

NUMBER OF COPIES: 200

## 43 GHZ, COOLED, LOW-NOISE AMPLIFIER

S. Weinreb, R. Harris, and M. Rothman

### 1.0. Introduction

This report describes construction details and measurement results of a four-stage amplifier designed for low noise in the 42 to 44 GHz range and an operating temperature of 17 K. Results concerning noise parameter measurements of four other HEMT devices at 300 K and 17 K are included.

### 2.0. Amplifier Description

An amplifier is comprised of an input tuner-transition, four single-stage carriers, an output tuner-transition, and a cover as shown in Figures 2.1-2.3. These components are described in this section.

#### 2.1. Tuner-Transition

The tuner-transition used at both input and output is a WR-22 waveguide E-plane T-junction. The input signal is applied to the arm of the T. A microstrip coupling probe and backshort is placed in one branch and a backshort (termed tee-short) is placed in the other branch. This configuration allows a known variable generator impedance to be presented at microstrip reference planes A and C of Figure 2.3 as the short positions are varied. The tuner-transition is described and analyzed in the MS thesis of M. Rothman [1]. The locus of impedance presented to a transistor chip as a function of backshort and tee-short positions is shown in Figure 2.4 for a frequency of 43 GHz and a substrate transformer of 19.5 ohm characteristic impedance.

There are two purposes of the variable tuner-transition. The first is to measure the four noise parameters of either a transistor device, a single-stage amplifier, or the four-stage amplifier. For this purpose backshorts which have position readouts and are movable through a non-translating rotary shaft as shown in Figure 2.1 are utilized. The second purpose is to provide the generator impedance which minimizes the amplifier noise temperature and load impedance which maximizes the amplifier gain. For this purpose a compact, semi-variable backshort is utilized.

The main drawing of the tuner-transition is shown in Figure 2.5, and a list of all drawings for the amplifier is given in Table 2.1.

#### 2.2. Chip Carrier and Quartz Substrates

Drawings of the chip carriers and quartz substrates are shown in Figures 2.6-2.8. The carriers are machined from copper and the substrates are made of crystalline quartz. The substrate material was chosen for its low dielectric constant (4.55) and thermal expansion coefficient close to that of copper. The linear contraction for quartz in the X-Y plane (specified as Z-cut crystalline quartz) is .244% compared to

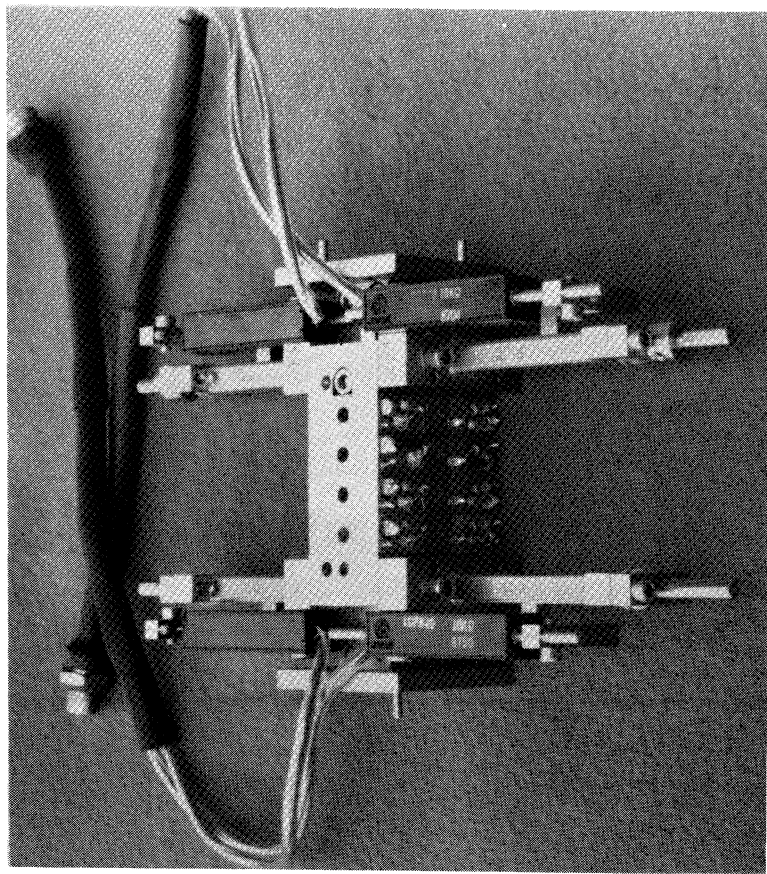
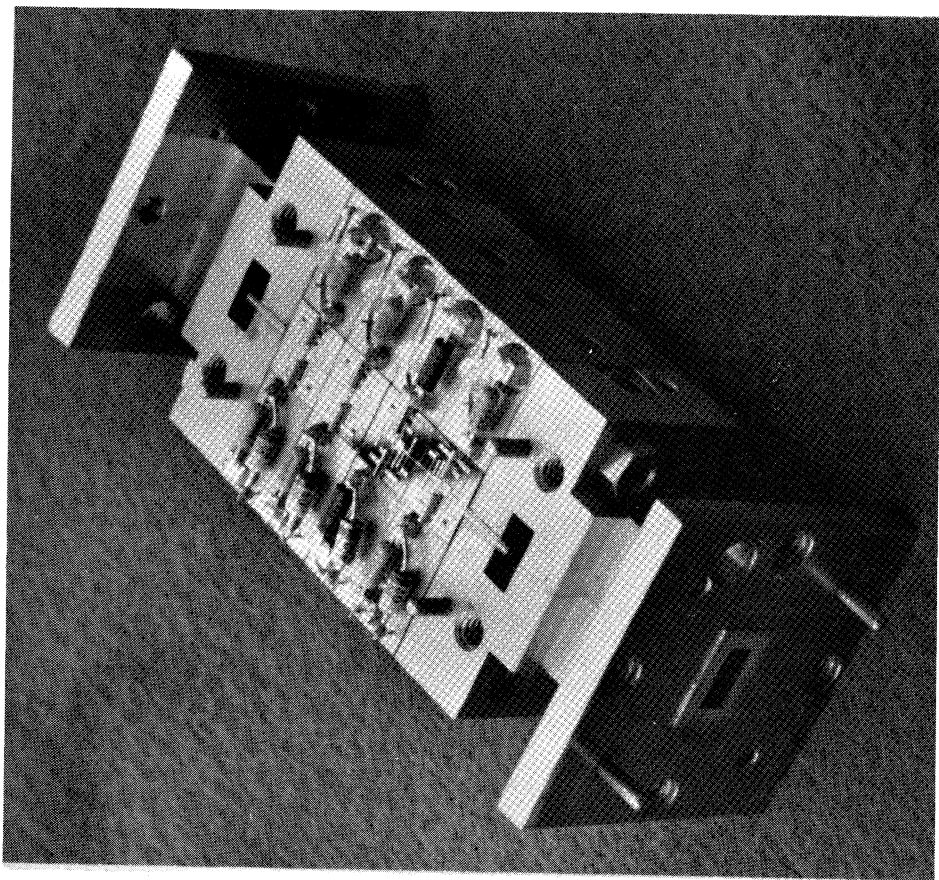


Fig. 2.1. Photograph of four-stage amplifier with input and output tuner-transitions including position readouts is shown at left while the amplifier with backshorts removed is shown at right.

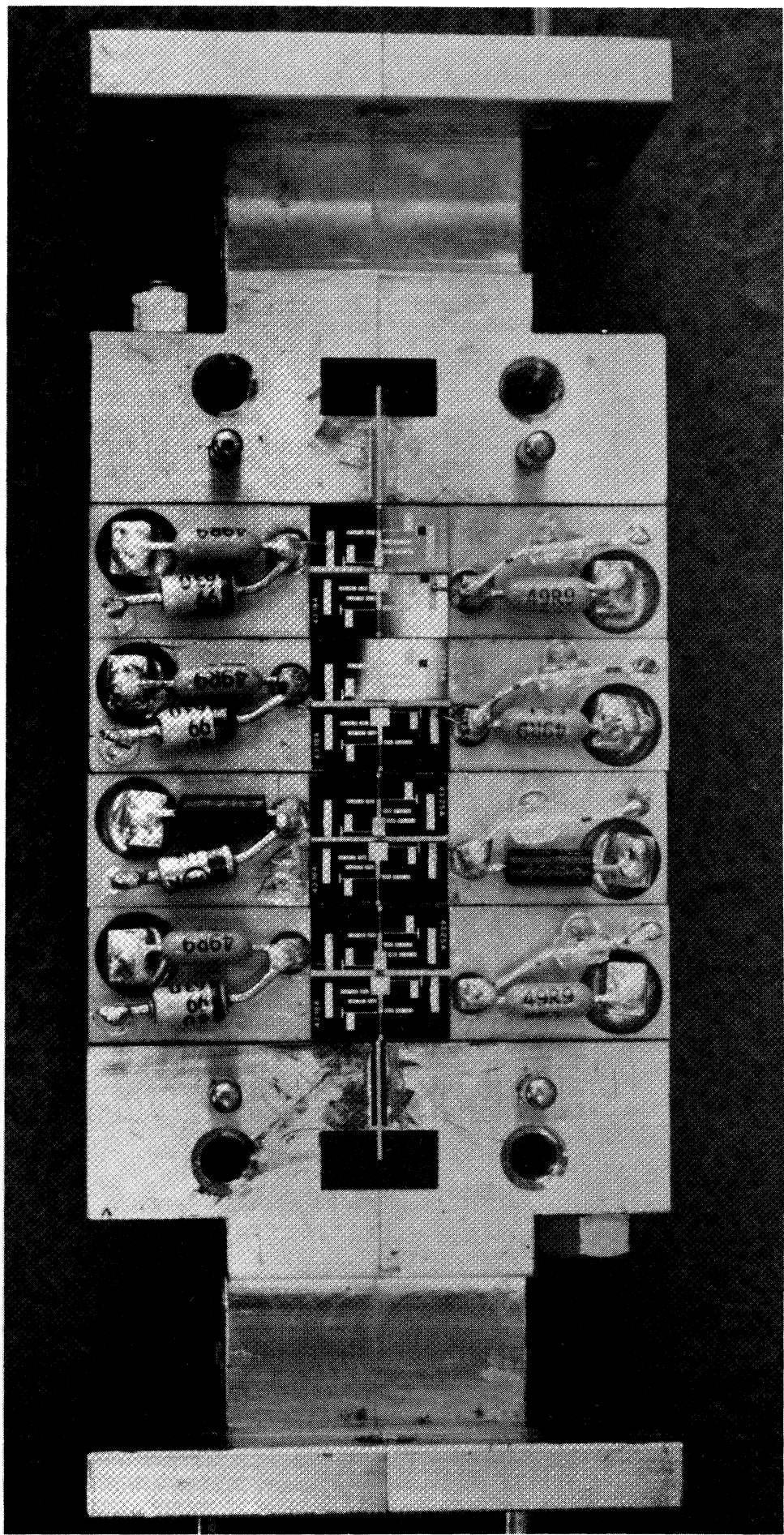
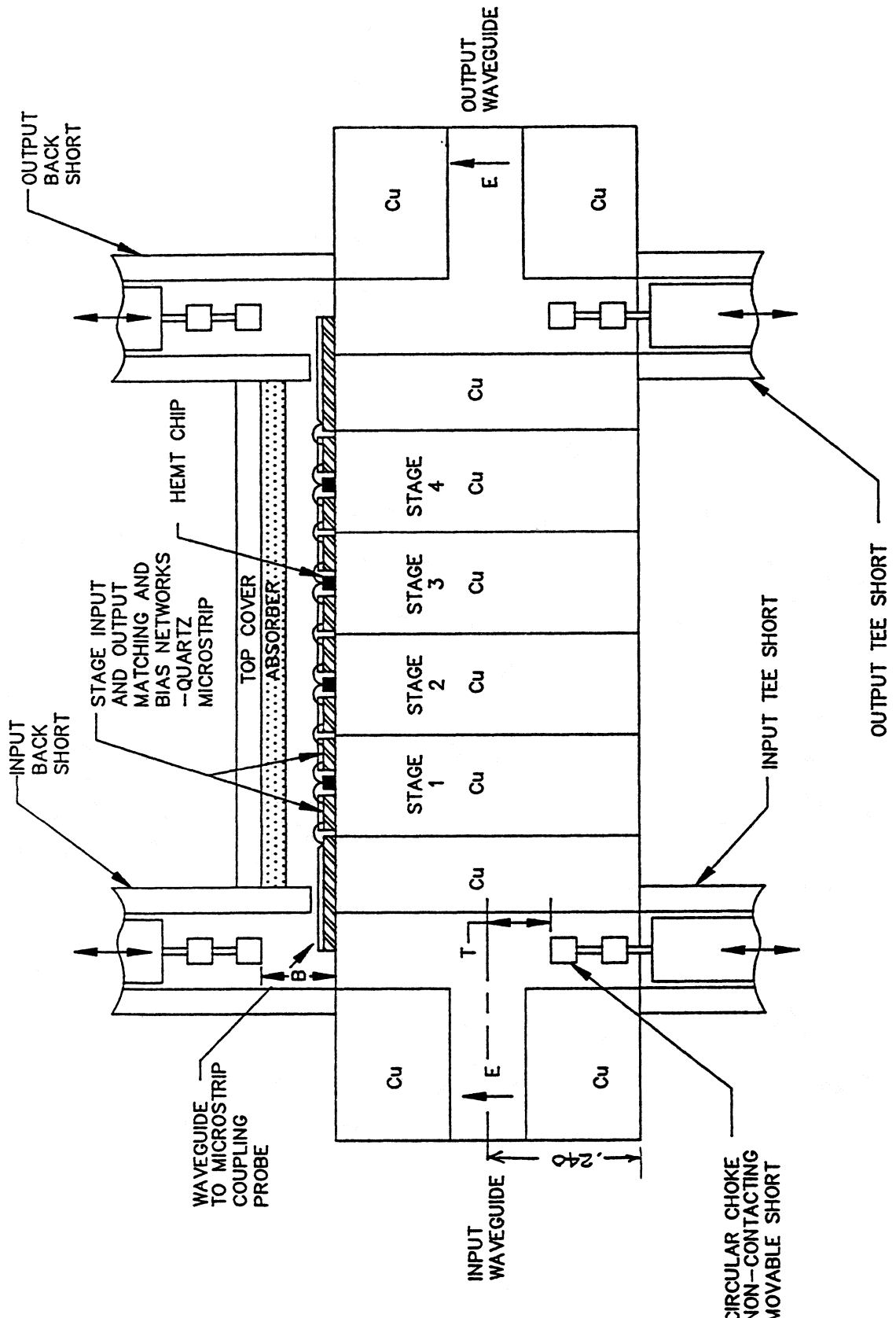


Fig. 2.2. View of four-stage, 43 GHz amplifier. Input is at left, drain bias circuits are at top, and gate bias circuits at bottom. Substrate material is .005" thick crystalline quartz.



**Fig. 2.3.** Cross-section view, not to scale, of complete four-stage amplifier including input and output tuner-transitions. The impedance at points A and C is known as a function of dimensions B and T. The backshort electrical position readouts give B and T directly (1 volt per inch).

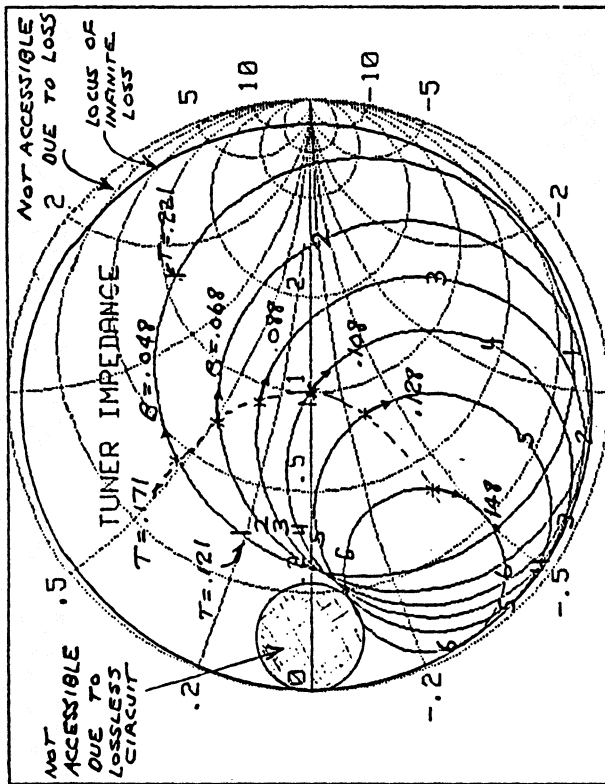
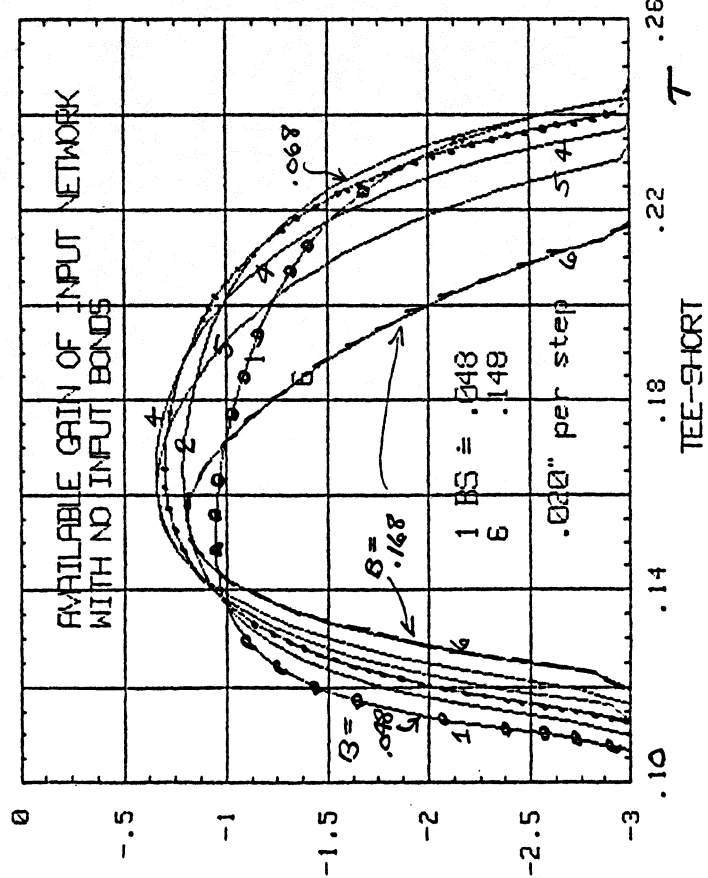
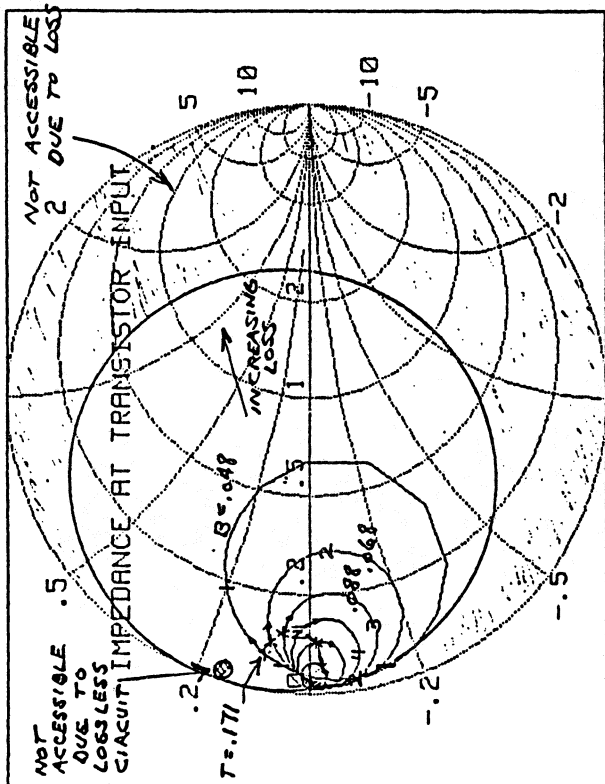
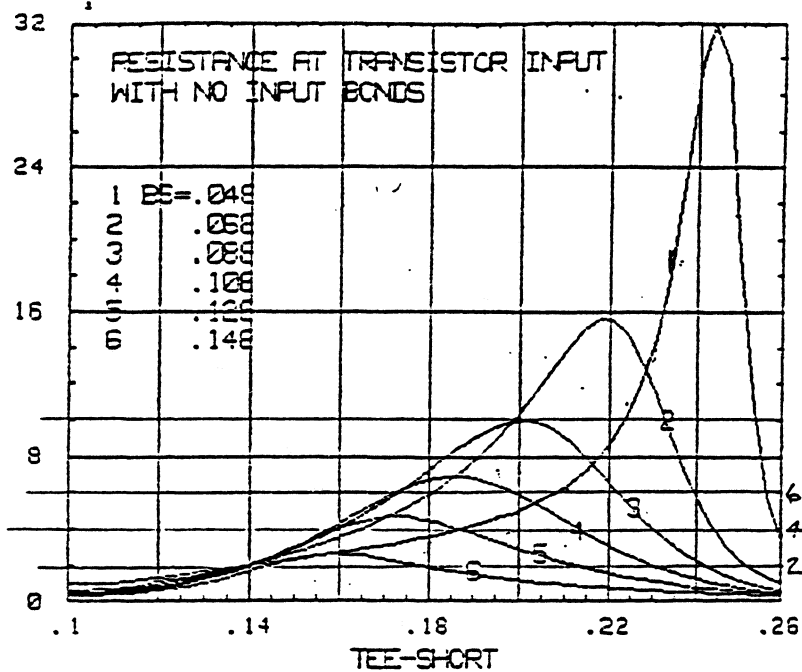


Fig. 2.4. (a) The locus of impedance at 43 GHz as a function of backshort position,  $B$ , for six values of tee-short position,  $T$ , is shown at top left for reference plane A (transition microstrip output) and at top right for reference plane C (facing transistor bond wire) assuming a 19.7 ohm  $\lambda/4$  transformer on the input substrate. At left the available gain (loss due to microstrip attenuation) is shown as a function of  $B$  and  $T$ . Results are from Rothman's thesis [1].





Z[22] I

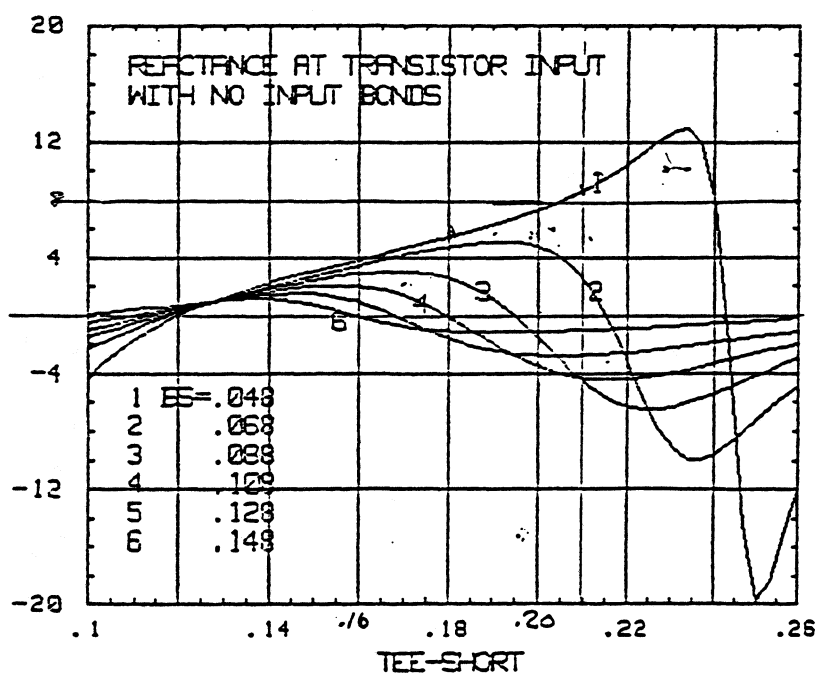


Fig. 2.4. (b) Resistance and reactance at bias-substrate to transistor-bond-wire interface for 19.7 ohm quarter-wave transformer.

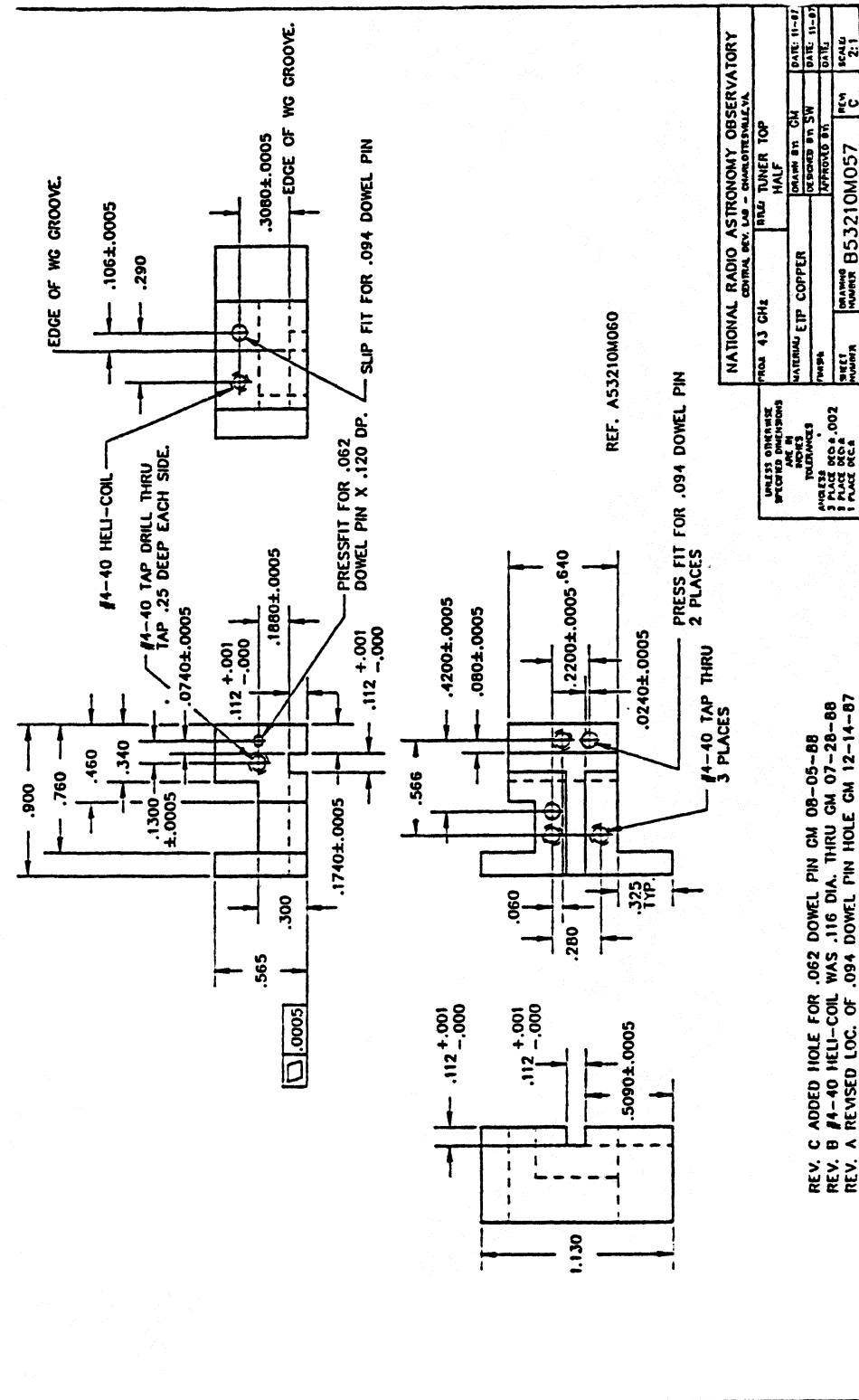


Fig. 2.5. Top half of tuner-transition. The bottom half is almost identical and the two halves join at a line which is not crossed by a current path.

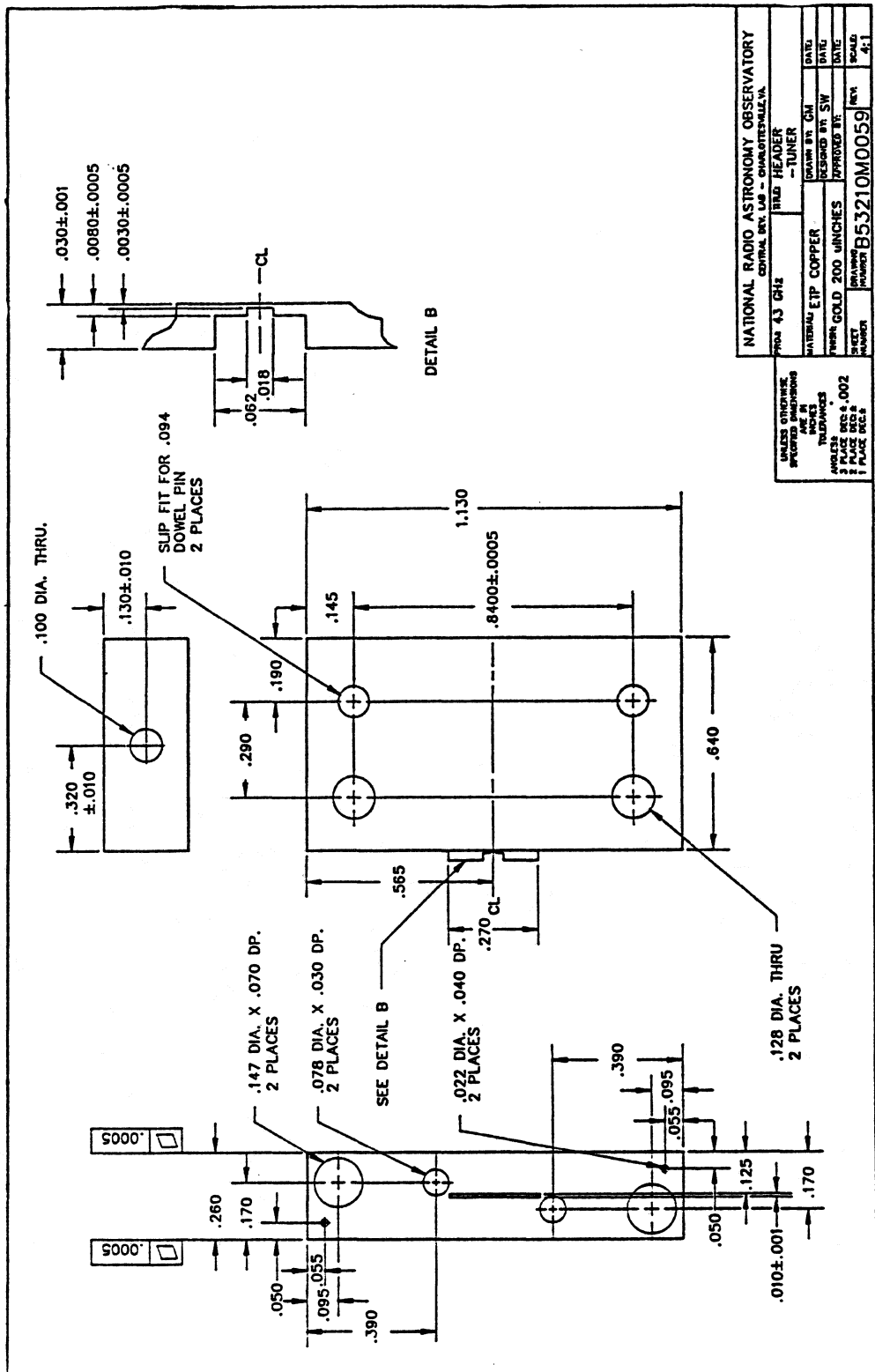


Fig. 2.6. Chip carrier (copper with 200  $\mu$ inch gold plate). The chip mounting area shown in detail B is dimensions for a .005" thick by .008" long by .012" wide transistor. These dimensions along with the carrier length (.260") must be varied to accommodate other chip sizes.

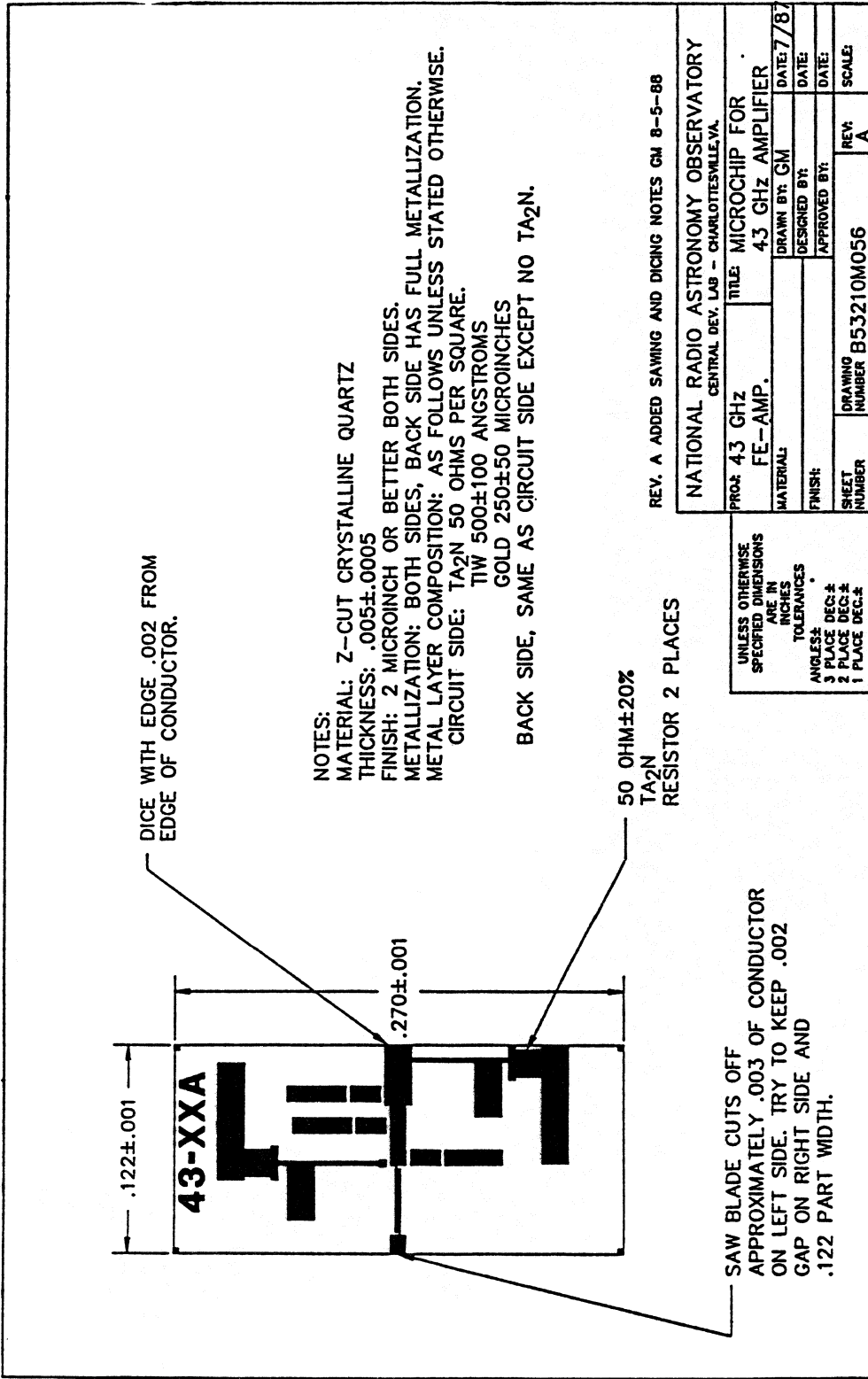


Fig. 2.7. Quartz substrate used for both input and output of each amplifier stage.

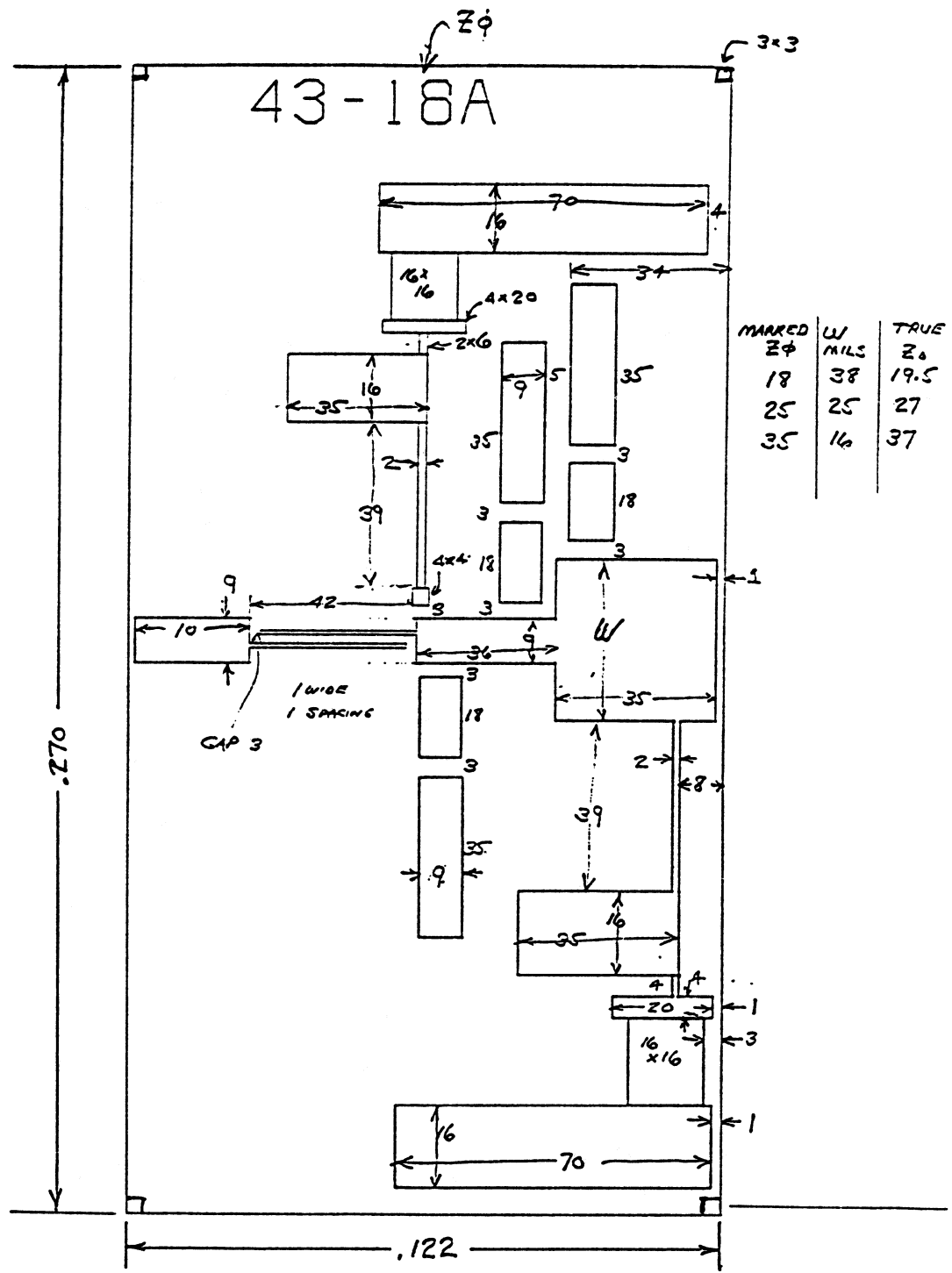


Fig. 2.8. Dimensioned (in units of .001") sketch of .005" thick crystalline quartz substrate. Substrates with three different values of W were fabricated; the  $Z_o = 19.5$  were used for input and  $Z_o = 27$  units were used for output.

TABLE 2.1. Drawings for 43 GHz Amplifier

**Tuner-Transition:**

<b>Tuner Top-Half*</b>	B53210M057
<b>Tuner Bottom-Half</b>	B53210M058
<b>Backshort Housing</b>	B53210M061
<b>WR22 Flange Detail Tuner</b>	A53210M060
<b>Drive Shaft</b>	A53210M062
<b>Waveguide Plug</b>	A53210M063
<b>Cap</b>	A53210M064
<b>Backshort Pin</b>	A53210M065
<b>Slider</b>	A53210M066
<b>Link</b>	A53210M067

**Chip-Carrier:**

<b>Header-Tuner</b>	B53210M059
---------------------	------------

**Substrate:**

<b>Microchip</b>	B53210M056
------------------	------------

\*Figure 2.5 of this report.

.325% for copper for a temperature change of 20C to -250C [2, pages 4-138 and 4-123]. Other metals which could be considered are nickel at .229% and iron at .204%.

The substrate was attached to the carrier with Epotek H20E [3] conductive epoxy. After several cool-downs (25C to -250C) of the four-stage amplifier (eight substrates), the bond of one substrate sheared and lifted off the carrier breaking the interstage bond wires. The shear appeared to be in the epoxy rather than in the adhesion to copper or quartz. In future amplifiers, a flexible conductive epoxy, Acme 3026 [4], is recommended. This epoxy is not very flexible at low temperatures, but it is more viscous and forms a thicker layer (~ .001") which can sustain greater shear strain.

One stage of the amplifier is shown in the schematic diagram shown in Figure 2.9 and detailed photographs are shown in Figures 2.10 and 2.11. Starting at the input at left, a coupled-line DC block as described by Bates [5] is used to block bias current and pass the RF signal as an equivalent section of 50 ohm transmission line. A number of capacitive  $\lambda/8$  or inductive  $3\lambda/8$  open-circuited stubs can then be bonded in at the points labeled 1A, 1B, . . . , 6B to produce a desired impedance transformation. The desired bonds were found by observing the gain while temporarily connecting the bond points with small pieces of gold ribbon bonded to a sharp toothpick. (Not very high-tech, but it worked!) It is also possible to bond at points 0 and 7 to add lossy low frequency terminations to increase stability to low-frequency oscillation. This was not found to be necessary since the bias circuit provides low-frequency termination. No B bonds were utilized and one to three wires were used at each bond point to give some finer tuning. The final arrangement of bonds is given in Table 2.2.

TABLE 2.2. Bond Wire Locations

	Point	Bonds
Stage 2	1A	2
	2A	3
	4A	3
Stage 3	2A	1
Stage 4	2A	3
	4A	1
	5A	3

In addition to these bonds, open-ended bond wires were attached to the center line with .018" length at point 2.5 of stage 1, .017" length at point 5 of stage 2, and .016" length at point 4.5 of stage 3. All stages utilized 19.5 ohm  $\lambda/4$  transformers at input and 27 ohm  $\lambda/4$  transformers at output.

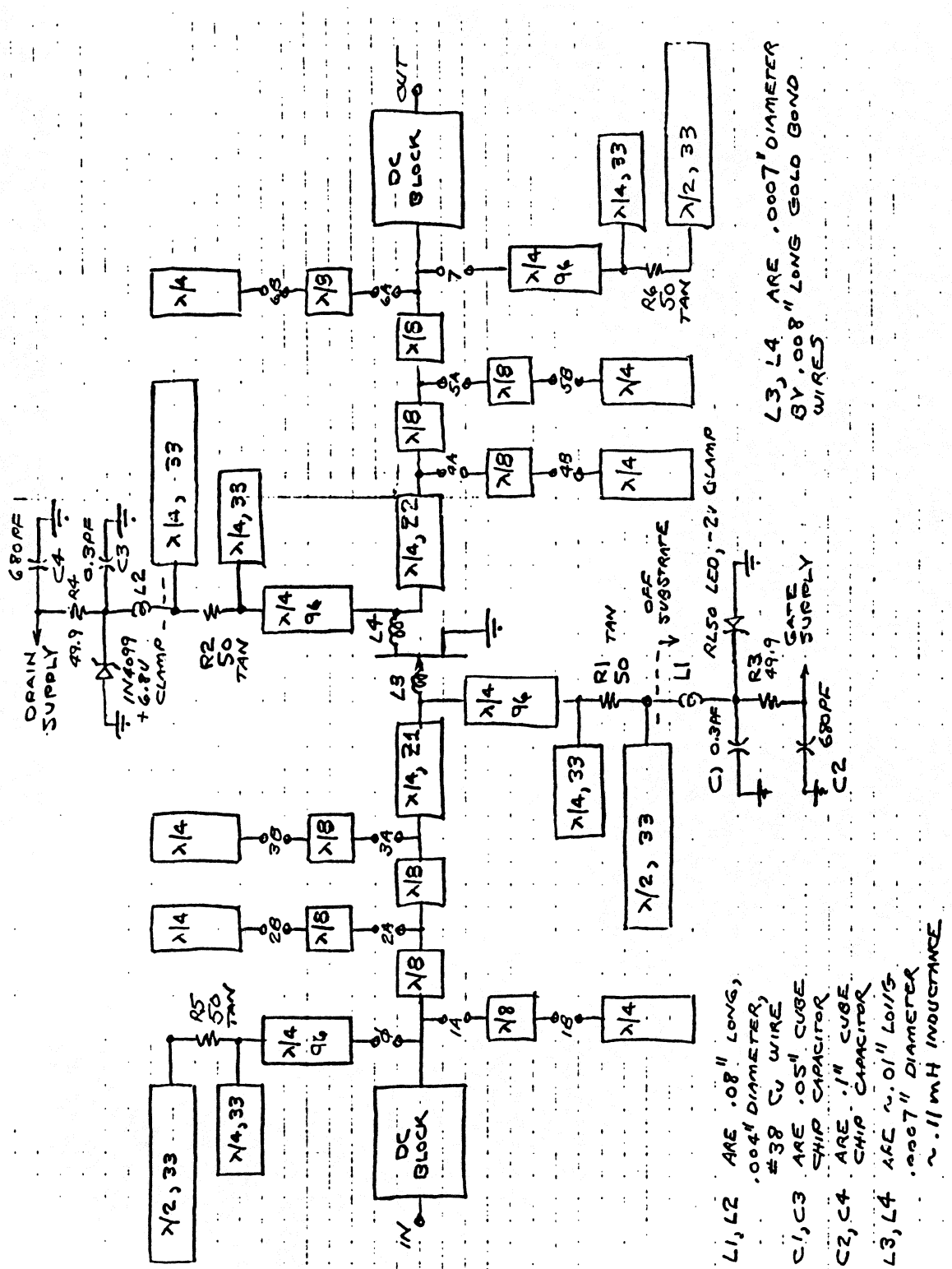


**Fig. 2.9.** Schematic diagram of an amplifier stage. The jumper locations 1A, 1B, . . . , 6B can be connected by bond wires to provide interstage matching. Jumpers 0 and 7 allow additional low-frequency stabilization networks to be connected. The jumpers used in the four-stage, prototype amplifier are specified in Table 2.2. Characteristic impedance is 50 ohms unless otherwise noted.

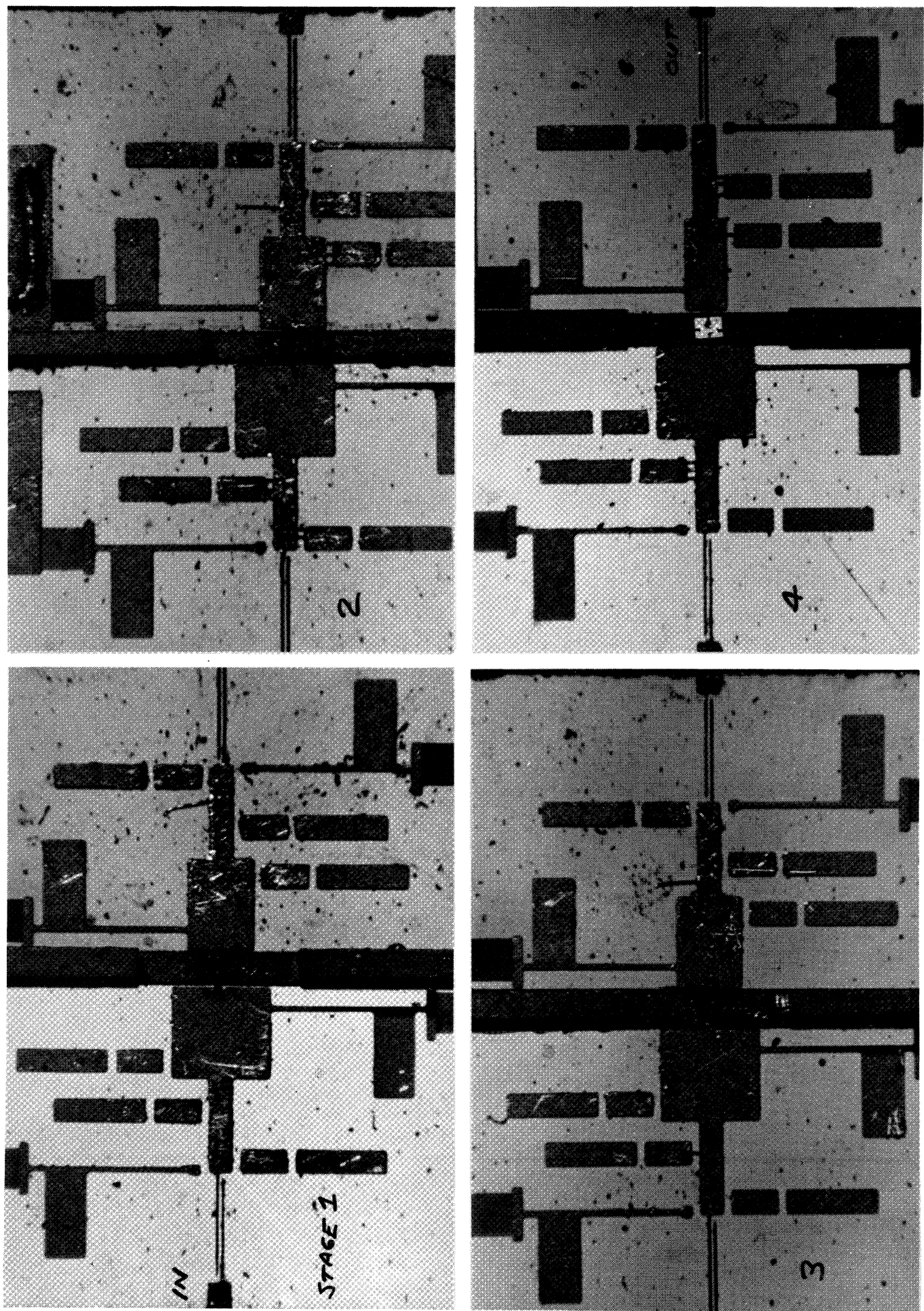


Fig. 2.10. Amplifier substrate photographs.



Fig. 2.11. Microscope photograph of stage three HEMT. For size reference the chip is .008" long (left to right in photo) by .012" wide. The bond wires are .7 mil diameter gold bonded at 105C stage temperature. The chip is attached with Epotek H20E epoxy.

### 3.0. Test Results

#### 3.1. Test Set

A block diagram and photograph of the test set used for noise, gain and reflection coefficient measurements are shown in Figures 3.1 and 3.2, respectively.

The test set and procedure are fairly conventional and will not be described except for the noise temperature calibration. The amplifier noise temperature is measured by turning on and off a noise diode (Noisecom NC5222) which is coupled into the amplifier through a 6 dB attenuator, 10 dB coupler, and directly at the amplifier, a coolable 10 dB waveguide attenuator. This final attenuator provides a low source temperature when cooled ( $0.9 \times 17 \text{ K} + 0.1 \times 300 \text{ K} = 45.3 \text{ K}$ ) and increases the accuracy of the noise measurement for an amplifier having noise temperature well under 300 K. As an example, for an amplifier with 50 K noise temperature, an error of  $\pm 5\%$  or  $\pm 0.2 \text{ dB}$  in noise source excess noise ratio ENR causes an error of  $\pm .05(300 + 50) = \pm 17.5 \text{ K}$  for a 300 K source temperature or  $\pm .05(45.3 + 50) = \pm 4.7 \text{ K}$  for the cooled 10 dB attenuator. In addition, the attenuator near the amplifier provides a more accurately determined source impedance.

The coolable attenuator was constructed by inserting in the waveguide a triangular vane of .012" thick crystalline quartz which had been metallized with nichrome having a resistivity of 400 ohms per square. The crystalline quartz has excellent thermal conductivity and was clamped to a copper bar. The temperature of the bar was monitored with a Lake Shore Cryogenics transducer and readout. The nichrome has negligible resistance change with temperature and a measurement of the total in dewar attenuation (amplifier replaced with waveguide jumper) gave  $0 \pm 0.2 \text{ dB}$  change of attenuation from 300 K to 17 K.

The ENR of the noise source including couplers and attenuators was measured at the reference plane of the amplifier input by comparing the noise from the source with that produced by a small conical horn. Microwave absorber (Emerson and Cuming AN72) at 300 K and 77 K (saturated with liquid nitrogen) was placed near the horn (exact location had negligible effect) and the receiver output was compared to that of the noise source. The comparison is facilitated with the NOISECALL program which performs the calibration as receiver frequency was scanned from 40.0 GHz to 45.0 GHz. The excess noise temperature of the noise source at the amplifier input plane was found to be 173 K (ENR = -2.24 dB) at 43 GHz and varied between 134 K and 174 K over the 40 to 45 GHz range. The noise source ENR was specified at +23.2 dB by the manufacturer and the total inserted nominal attenuation ( $6 + 10 + 10 = 26 \text{ dB}$ ) would give an ENR of  $\sim -2.8 \text{ dB}$  without consideration of  $\sim 1 \text{ dB}$  of extra losses. It thus appears that the noise source manufacturer's ENR is  $\sim 1.6 \text{ dB}$  too high, but accurate loss measurements would be needed to verify this.

The output of the program NOISECALL is a table of ENR vs. frequency; this table was then incorporated into the NOISE1 program (a

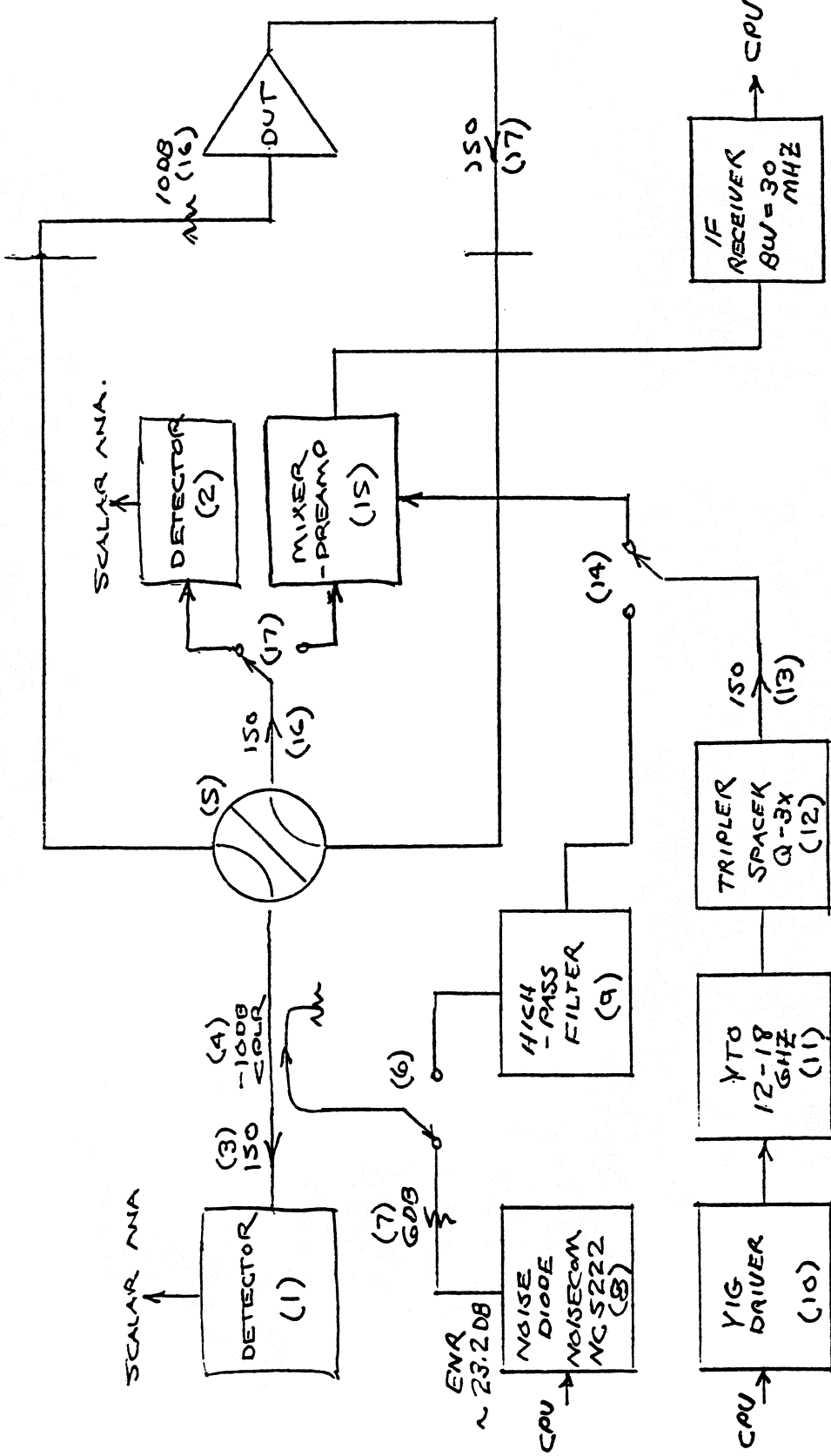


Fig. 3.1. Test set for noise, gain, and reflection coefficient measurements. The switches are shown in the position used for gain and noise measurements in conjunction with an Apple II computer and programs NOISECALL and NOISE1. By throwing switches (6) and (14) to the alternate position swept-frequency gain and return loss measurements are made in conjunction with a Wiltron 560 scalar analyzer. The attenuator (16) is only used for cooled amplifier noise measurements and increases the accuracy of measurement. Switch (5) allows bypassing or reversing the device under test.

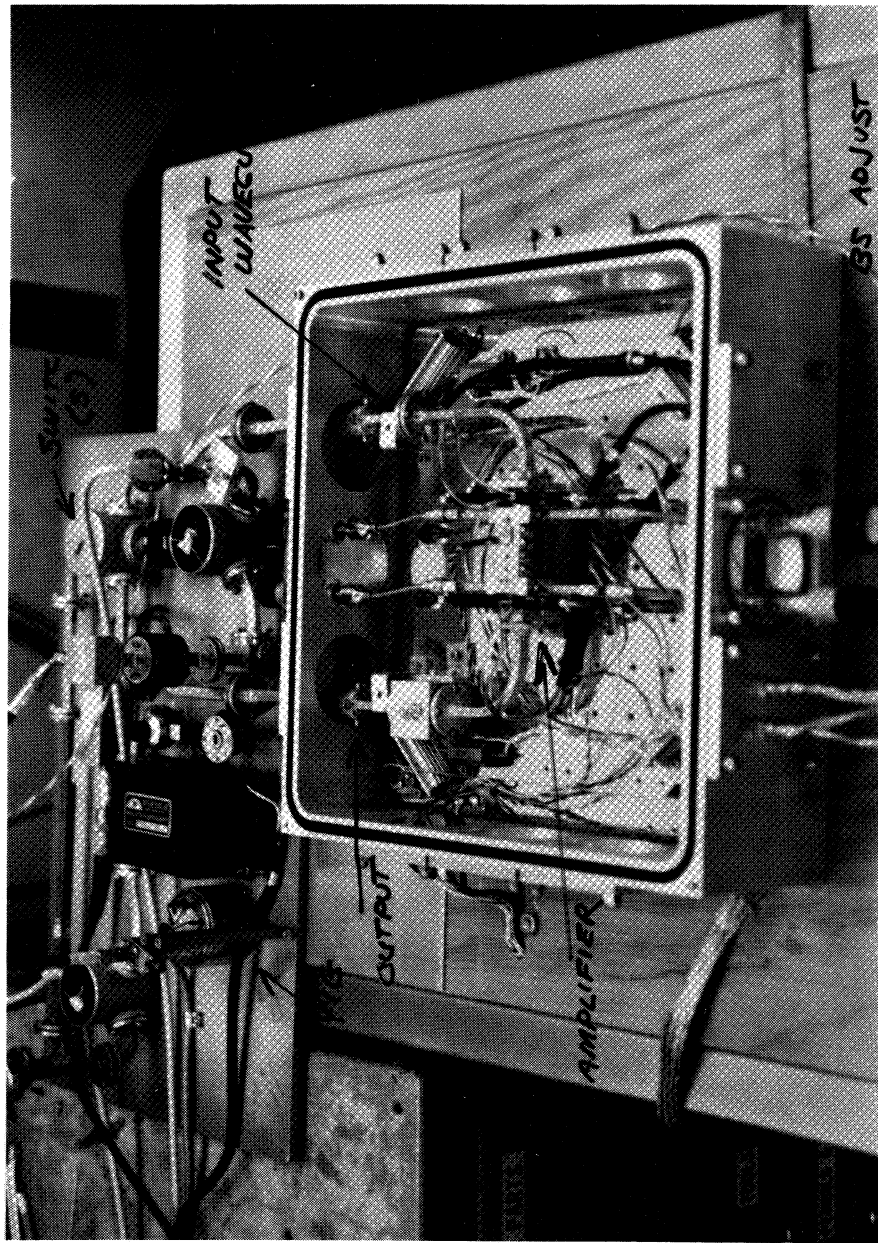


Fig. 3.2. Photograph of cryogenic test configuration with dewar cover removed. The amplifier with tuners, input attenuator (not present in this photo), and output isolator is cooled to  $\sim 17$  K by a CTI Model 1020 refrigerator. Gapped waveguides are used for the 300 K to 17 K thermal transitions.

special version labeled NOISE1B) which measures amplifier noise applying a correction for the measured test receiver noise.

### 3.2. Four-Stage Amplifier Results

An amplifier was constructed as described in Section 2 utilizing experimental HEMT devices provided by George Duh of the General Electric Electronics Laboratory, Syracuse, NY. The devices in the first three stages are similar to those used in the Neptune/Voyager 8.4 GHz receivers with the exception of narrow gate width ( $75 \mu\text{m}$  rather than  $300 \mu\text{m}$ ) and 3% higher aluminum mole fraction in the AlGaAs layer. This higher mole fraction was not desirable and caused high light sensitivity and past-history dependence at cryogenic temperatures. The devices had  $0.25 \mu\text{m}$  gate length, are from wafer 392, are described in a paper by Duh, et al. [6], and have S-parameters as given in Table 3.1. The amplifier's fourth stage utilized a  $0.1 \mu\text{m}$  gate length experimental GE HEMT which, in early tests, was not as low noise as the newer  $0.25 \mu\text{m}$  devices.

The measured gain and noise of the four-stage amplifier at 300 K and 17 K are given in Figure 3.3 and variations with first stage bias values are described in Figures 3.4 and 3.5.

The four noise parameters of an amplifier can be measured by measuring the noise temperature at  $\geq 4$  values of source impedance as determined by  $\geq 4$  settings of the input tuner. This has been performed for the amplifier at 300 K and 17 K for five tuner positions with raw data and analysis results shown in Figure 3.6. The noise temperature is corrected for conductor loss in the input substrate; this loss is a function of tuner setting (see Figure 2.4) and ranges between 0.5 and 1.9 dB. These figures are theoretical calculations and are for a temperature of 300 K. At cryogenic temperatures the loss will decrease by an amount dependent on conductor purity; a decrease by a factor of 0.5 has been estimated. The loss correction decreases the minimum noise temperature from 479 K to 348 K at room temperature and from 43 K to 38 K at cryogenic temperature.

The noise parameters are calculated using an Apple II BASIC program, NPF 880803, which utilizes the method of Caruso and Sannino [7] to find the best-fit values. The value of  $R_{\text{opt}}$  decreases from  $10.6 \pm 1.6 \Omega$  at 300 K to  $6.9 \pm 0.5 \Omega$  at 17 K. The values of  $X_{\text{opt}}$  of  $-4.7 \pm 1.6 \Omega$  at 300 K and  $-3.6 \pm 0.6 \Omega$  at 17 K include the bond wire reactance which is estimated to be  $30 \pm 10$  ohms. The value of  $X_{\text{opt}}$  at the transistor chip is thus  $\sim 26 \Omega$  which resonates a capacitance of  $0.14 \text{ pF}$ . The error limits on the above quantities are calculated from numerical derivatives computed by the program. The error limit is based upon a  $\pm 10\%$  error in measurement of the noise temperature which has greatest effect upon the noise parameter.

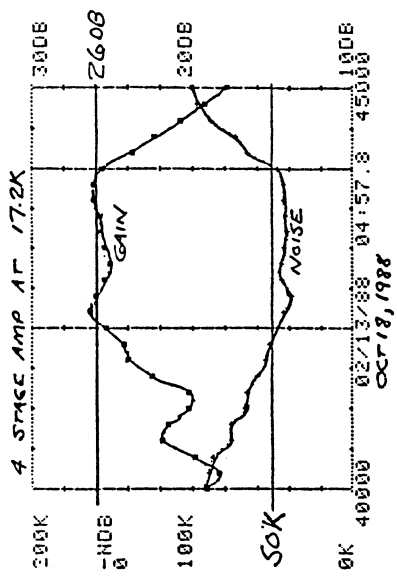
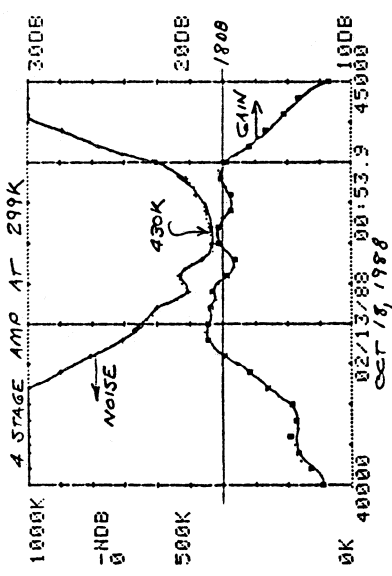
### 3.3. Transistor Tests

Other transistors were tested as single-stage amplifiers utilizing the test set and procedure that have been described. Results are summarized in Table 3.2.

1) 300K OFT .@98,.192,.096,.17E  
 $\nu_0: 53.9$  02/13/88 TAV=5.05.4 TL0=429.3 @ 430000 GL=17.2  
 $\nu_{o1}/\nu_{p1}$

2. @1.5,-.058 2. @1.5.1,.088 3. @1.6.9,.28 3. @1.7.2,..

1) FINAL OFT .1@d,.2@b,.11@,.16@  
 $\nu_0: 57.8$  02/13/88 TAV=4.3 TL0=37.7 @ 424@ GL=25.1 GH=26.3  
 $\nu_o - \nu_{G1}$   
 $\nu_{o1},2,-,\nu_{G2}$  2. @1.2.1,.@11 3. @1.4,.231 3. @1.7.1,.413  
 $\nu_{o2} - \nu_{G3}$



F, GHz	NOISE GAIN,DB	F, GHz	NOISE GAIN,DB
41. @0.0	11@7.4	41.2@0	1@14.2
41.4@0	897.9	16.3	17.9
41.8@0	7@3.4	18.8	18.9
42.2@0	597.9	18.7	42.4@
42.6@0	529.8	17.7	42.8@
43.0@0	429.3	18.1	43.2@
43.4@0	448.5	17.5	43.6@
43.8@0	506.9	18.1	44.0@
44.2@0	78@.3	16.4	44.4@
44.6@0	1@3@.1	14.2	44.8@

F, GHz	NOISE GAIN,DB	F, GHz	NOISE GAIN,DB
41. @0.0	66.8	2@.1	41.2@
41.4@0	59.0	22.4	41.6@
41.8@0	51.3	24.2	42.0@
42.2@0	43.2	26.3	42.4@
42.6@0	44.7	25.4	42.8@
43.0@0	42.6	25.5	43.2@
43.4@0	41.6	25.7	43.6@
43.8@0	43.7	26.1	44.0@
44.2@0	65.6	23.6	44.4@
44.6@0	87.5	2@.7	44.8@

Fig. 3.3. Noise temperature and gain of four-stage amplifier at 299 K (left) and 17.2 K (right). The noise temperature is referred to the amplifier input flange (at 17.2 for the cooled amplifier) and includes the effect of input tuner and substrate loss.

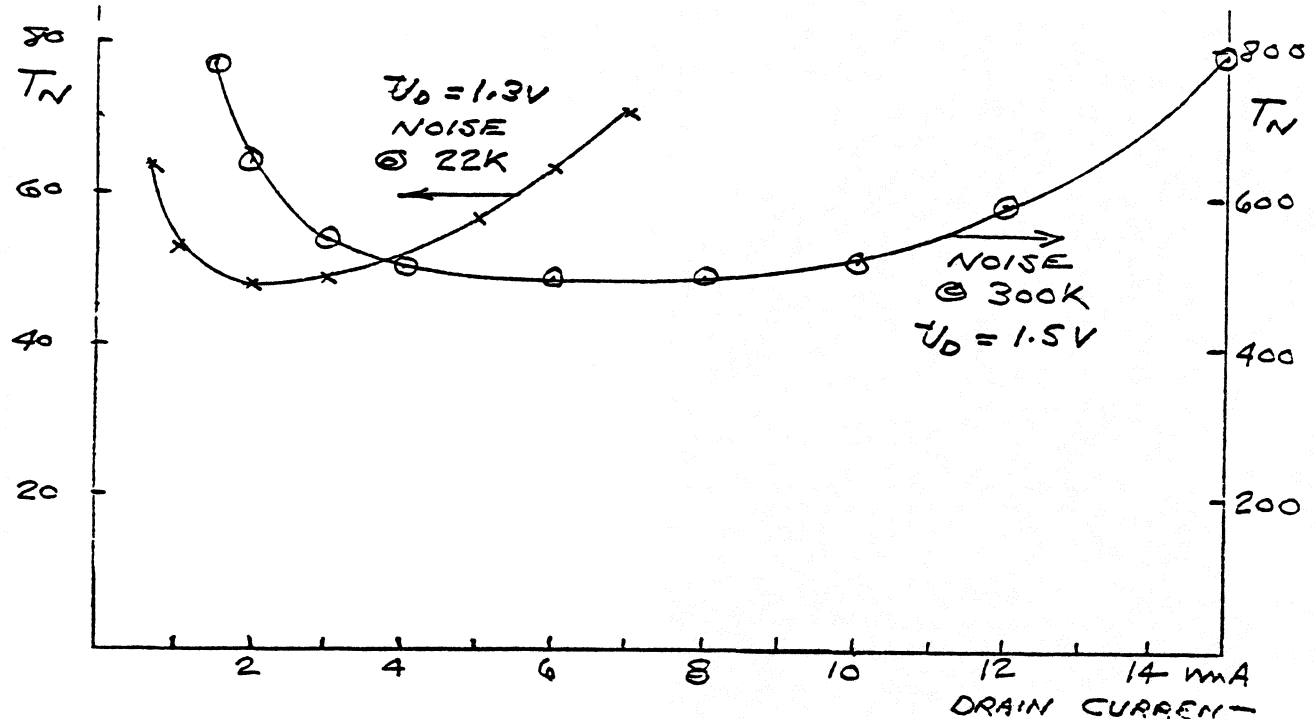


Fig. 3.4. Noise temperature at 43 GHz vs. stage 1 drain current for amplifier at 22 K and at 300 K. The input tuner setting was held constant at each temperature and was not very different at the two temperatures. The maximum gain was 19.0 dB at 10 mA at 300 K and 25.2 dB at 7 mA at 22 K. Note that the DC power required at optimum noise bias is 2.6 mW at 22 K and 9 mW at 300 K.

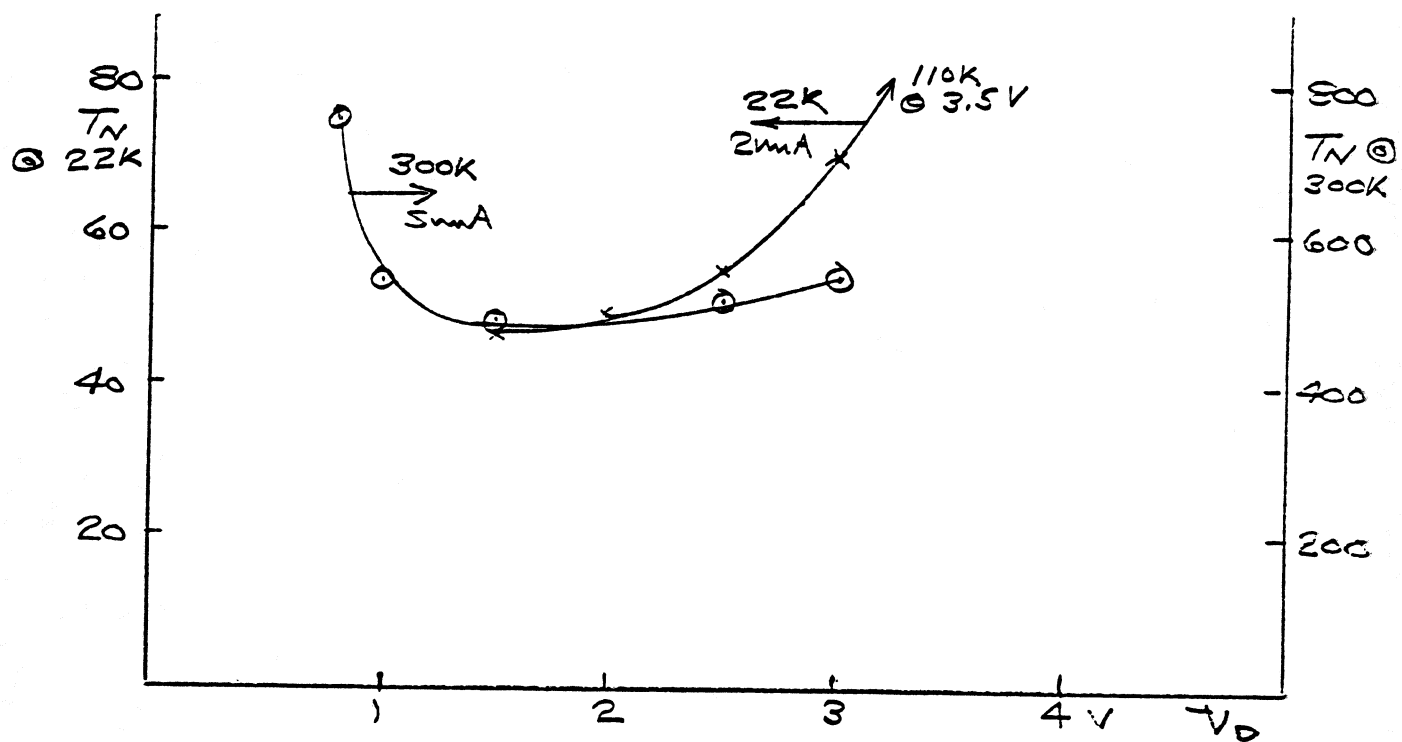


Fig. 3.5. Noise temperature vs. stage 1 drain voltage at 300 K and 22 K. After increasing drain voltage to 3.5 V at 22 K, the noise temperature measured at 1.5 V increased by 5 K and required gate voltage for 2 mA drain current changed from -.061 V to -.123 V. Turning bias off and on brought the gate bias to -.098 V with little change in noise temperature. After warming up to 300 K and cooling again, the original noise temperature and gate voltage were obtained.

DEVICE A STAGE 110 NOISE										12 K		17 K	
Condition	TUNER IN 0.5	TUNER OUT 0.5	F GHZ	T K	G 0.5	R <sub>S</sub>	X <sub>S</sub>	ANALYSIS NO. 88-023	T G	ANALYSIS NO. 88-023	T G		
29 K	.102	.200	.109	.163	43	479	18.5	9.6	-4.7	T <sub>MIN.</sub> 36.8 <sup>1</sup>	348	168	-0.3
0.145, 2.5, -0.67	.102	.229			111	17.1	3.5	-7.0	R <sub>OPP</sub> 15.6	612	354	-1.9	
2.5, + 0.85													
3.7, + 2.90	.102	.152			835	17.0	3.9	2.0	X <sub>OPP</sub> -4.7	712	108	-0.5	
3.7, + 4.54													
.141	.200				1217	17.1	2.1	-3.2	G <sub>N</sub> 0.45 <sup>2</sup>	800	275	-1.4	
.063	.200				699	16.4	10.5	7.4	N	.48	531	168	-0.8
9.15, 17 K	.102	.200	.110	.163		43	25.6	9.6	-4.7	T <sub>MIN.</sub> 39	38	.68	-0.8
1.5, 2, -0.53						81	24.7	3.5	-7.0	R <sub>OPP</sub> 15.9	64	17	-1.9
2, 2, .011	.102	.229											
3, 4, + 2.32	.102	.152			81	23.7	3.9	2.0	X <sub>OPP</sub> -3.6	76	354	-0.5	
3, 7, + 4.12													
.141	.200				80	25.1	2.1	-3.2	G <sub>N</sub> 0.61 <sup>3</sup>	66	14	-1.4	
.063	.200				81	22.7	10.5	7.4	N	.07	73	.68	-0.8
OUTPUT TUNER	.109	.163	AT PROBE MICROSTRIP REFERENCE PLANE	70		38	4						
INPUT TUNER	.102	.200				70	-41						
(1)	(2)	(3)	(4)	(5)	(6)	(7)	(8)	(9)	(10)	(11)	(12)	(13)	(14)

Fig. 3.6. Raw data and analysis of measurements to determine noise parameters of four-stage amplifier at 300 K and 17 K. The tuner positions in columns (2) and (3) are used to calculate the source impedance (9) and (10), and tuner available gain (13) using analysis presented by Rothman [1]. The available gain is used to calculate a corrected noise temperature (12) and finally best-fit noise parameters (11).

TABLE 3.1. Signal Parameters of GE 392 .25 x .75 μm HEMT

392 .5 .75(1) VD=2 VG=.06 ID=.4 m  
 CORRECTED DATA, SYMMETRIC MODEL  
 REFERENCE PLANE = .208

FREQUENCY GHZ	RETURN LOSS-IN		LOSS-FORWARD		LOSS-REVERSE		RETURN LOSS-OUT		FREQ(GHz)	K	Gu(dB)	MAG(dB)	MSG(dB)	H21
	MAG	ANG	S11	S21	MAG	ANG	S12	MAG	ANG					
2.00	.996	-7.2	1.968	169.7	.017	83.2	.809	-8.5	2.00	.07	36.68	***	20.53	20.50
2.50	.995	-9.4	1.955	167.0	.022	81.5	.809	-10.7	2.50	.09	38.08	***	19.58	15.51
3.00	.991	-11.6	1.945	164.2	.025	79.9	.887	-12.6	3.00	.11	33.88	***	18.85	12.40
3.50	.987	-13.9	1.962	161.5	.029	77.9	.886	-14.5	3.50	.13	31.90	***	18.30	10.39
4.00	.982	-16.3	1.970	158.9	.032	76.3	.802	-16.4	4.00	.16	29.71	***	17.83	8.94
4.50	.976	-18.6	1.961	156.4	.036	74.4	.797	-18.2	4.50	.19	27.17	***	17.41	7.81
5.00	.971	-20.8	1.958	154.0	.038	72.9	.793	-19.9	5.00	.21	26.64	***	17.08	6.99
5.50	.969	-22.9	1.973	151.8	.041	71.3	.791	-21.6	5.50	.21	26.97	***	16.81	6.42
6.00	.971	-24.8	1.973	149.6	.044	69.7	.790	-23.3	6.00	.20	29.45	***	16.52	5.92
6.50	.972	-27.1	1.982	147.2	.046	68.0	.790	-24.7	6.50	.20	33.47	***	16.33	5.43
7.00	.971	-29.1	1.991	144.7	.048	66.2	.789	-26.0	7.00	.21	32.74	***	16.16	5.08
7.50	.966	-31.1	1.976	142.2	.050	64.5	.783	-27.5	7.50	.24	28.19	***	15.95	4.75
8.00	.956	-32.8	1.974	140.3	.052	63.1	.777	-29.0	8.00	.20	25.08	***	15.76	4.55
8.50	.948	-34.2	1.978	138.5	.055	61.8	.771	-30.5	8.50	.31	23.64	***	15.57	4.42
9.00	.945	-35.7	1.994	136.7	.058	60.0	.767	-32.5	9.00	.31	23.12	***	15.38	4.31
9.50	.944	-37.4	2.027	134.5	.061	58.0	.764	-34.8	9.50	.31	23.16	***	15.23	4.22
10.00	.944	-39.5	2.052	132.0	.064	56.0	.762	-36.9	10.00	.31	23.53	***	15.06	4.07
10.50	.946	-42.1	2.106	129.2	.068	53.8	.761	-39.2	10.50	.30	25.08	***	14.91	3.95
11.00	.945	-45.1	2.136	126.1	.073	51.3	.762	-41.8	11.00	.29	26.75	***	14.68	3.76
11.50	.927	-49.2	2.197	121.9	.077	47.9	.749	-45.1	11.50	.34	23.61	***	14.56	3.64
12.00	.917	-52.5	2.172	118.8	.082	44.9	.745	-47.8	12.00	.36	22.08	***	14.22	3.43
12.50	.903	-55.6	2.174	116.2	.087	42.5	.733	-50.5	12.50	.38	20.94	***	13.99	3.32
13.00	.901	-58.9	2.212	113.7	.093	40.2	.732	-53.6	13.00	.36	22.10	***	13.78	3.25
13.50	.908	-62.8	2.266	110.0	.100	36.9	.732	-57.0	13.50	.33	24.32	***	13.56	3.15
14.00	.910	-67.0	2.282	105.7	.105	33.0	.726	-60.1	14.00	.34	24.46	***	13.36	3.01
14.50	.906	-71.1	2.274	101.8	.111	30.1	.719	-62.9	14.50	.34	25.04	***	13.13	2.88
15.00	.895	-75.4	2.273	98.0	.116	26.7	.709	-66.2	15.00	.36	23.82	***	12.92	2.79
15.50	.889	-79.2	2.254	94.3	.121	23.8	.695	-69.4	15.50	.39	22.51	***	12.70	2.71
16.00	.861	-81.6	2.238	91.6	.126	21.4	.683	-72.7	16.00	.41	20.53	***	12.51	2.70
16.50	.857	-83.7	2.246	89.3	.131	19.1	.673	-75.9	16.50	.41	20.33	***	12.34	2.70
17.00	.864	-86.4	2.309	87.0	.139	17.2	.669	-78.9	17.00	.38	23.13	***	12.21	2.73
17.50	.875	-89.4	2.367	83.6	.146	14.3	.673	-81.8	17.50	.37	27.29	***	12.09	2.72
18.00	.866	-93.6	2.407	79.1	.154	11.1	.660	-84.7	18.00	.39	26.74	***	11.94	2.69
18.50	.833	-98.2	2.399	75.2	.159	8.1	.634	-86.6	18.50	.45	20.86	***	11.80	2.66
19.00	.815	-103.8	2.373	71.6	.162	5.3	.601	-88.0	19.00	.48	19.39	***	11.66	2.58
19.50	.800	-108.7	2.377	68.8	.168	3.0	.574	-89.2	19.50	.50	18.54	***	11.51	2.54
20.00	.802	-115.9	2.425	65.0	.175	-4	.546	-89.7	20.00	.51	18.69	***	11.43	2.47

TABLE 3.2. HEMT 43 GHz Noise Parameter Summary - December 6, 1988

MFG	GE	FUJITSU	LIN MONO	LIN MONO
TYPE #	391	FHR10X	HCF502	HCF1006
REFERENCE	[3]	-	[4]	[4]
GATE DIM	.25 x 75	.25 x 100	.1 x 50	.1 x 100
<b>300 K DATA</b>				
V <sub>D</sub> , I <sub>D</sub> OPT	1.4, 6	2, 7	1.3, 7	1, 10
V <sub>g</sub> , G <sub>m</sub>	-.039, 27	-.332, 33	-.572, 20	-.580, 42
T <sub>min</sub>	120 ± 15	277 ± 30	195 ± 66	103 ± 8
R <sub>opt</sub>	5.2 ± 0.7	13 ± 6	10 ± 3	4.9 ± 2.4
X <sub>opt</sub>	8.0 ± 0.8	1 ± 6	24 ± 6	8.7 ± 1.1
N	.39 ± .08	-	.22 ± .1	.13 ± .06
G <sub>a</sub> (dB)	5.0	3.7	6 ± 1	6.7
T <sub>casc</sub>	175 ± 22	483 ± 50	259 ± 90	131 ± 10
<b>17 K DATA</b>				
V <sub>D</sub> , I <sub>D</sub> OPT	1.35, 1.5	2.5, 5	0.8, 2	1.8, 2
V <sub>g</sub> , G <sub>m</sub>	-.135, 24	-.479, 39	-.736, 16	-.896, 30
T <sub>min</sub>	27 ± 2	36 ± 8	34 ± 7	25 ± 1.0
R <sub>opt</sub>	6.5 ± 1	14 ± 6	8 ± 5	5.3 ± 0.3
X <sub>opt</sub>	4.3 ± 0.6	-3 ± 6	21 ± 4	3.7 ± 0.4
N	.07 ± .03	-	.03 ± .02	.04 ± .003
G <sub>a</sub> (dB)	5 ± .5	5.6	6 ± 1	6.9
T <sub>casc</sub>	39 ± 5	50 ± 12	45 ± 15	31 ± 1

## REFERENCES

- [1] M. Rothman, "Calibrated Tuner for Millimeter-Wave Device Calibration," MS Thesis, Department of Nuclear Engineering and Engineering Physics, University of Virginia, Charlottesville, VA, December 1988.
- [2] American Institute of Physics, AIP Handbook, 3<sup>rd</sup> edition, McGraw Hill, 1972.
- [3] Epoxy Technology, Inc., 14 Fortune Drive, Billerica, MA 01821, (617) 667-3805.
- [4] Acme Chemicals, P. O. Box 1404, New Haven, CT 06505, (203) 562-2171.
- [5] Bevan Bates, "Design of a Microstrip DC Block," Electronics Division Internal Report No. 276, NRAO, Charlottesville, VA, February 1988.
- [6] K. H. G. Duh, M. W. Pospieszalski, W. F. Kopp, P. Ho, A. A. Jabra, P. C. Chao, P. M. Smith, L. F. Lester, J. M. Ballingall and S. Weinreb, "Ultra-Low-Noise, Cryogenic, High-Electron-Mobility Transistors," *IEEE Trans. Electron Devices*, vol. 35, pp. 249-256, March 1988.
- [7] Giuseppe Caruso and Mario Sannino, "Computer-Aided Determination of Microwave Two-Port Noise Parameters," *Trans. on Microwave Theory & Tech.*, vol. MTT-26, no. 9, pp. 639-641, September 1978.
- [8] R. E. Lee, R. S. Beaubien, R. H. Norton and J. W. Bacon, "Ultra-Low-Noise, Millimeter-Wave HEMT's," submitted to 1989 MTT-S International Microwave Symposium.